PERGAMON

Available online at www.sciencedirect.com

SCIENCE DIRECT®

International Journal of Heat and Mass Transfer 47 (2004) 35–42

International Journal of HEAT and MASS TRANSFER

www.elsevier.com/locate/ijhmt

The LDA study of flow gas-dynamics in a vortex chamber

E.P. Volchkov *, V.P. Lebedev *, V.V. Lukashov

S.S. Kutateladze Institute of Thermophysics, Siberian Branch of Russian Academy of Sciences, 630090 Novosibirsk, Russia

Received 12 May 2003; received in revised form 24 June 2003

Abstract

The experimental data on the turbulent structure of swirling flow in vortex chamber with diaphragm are presented. The data were made with the help of LDA method. The evolution of turbulence intensity in the vortex chamber is shown. The influence of initial conditions of the swirling flow forming on the turbulent properties are considered.

Keywords: LDA measurement; Swirling flow; Turbulence

1. Introduction

Swirl flows are widely used in various technical devices and technological processes, for example, to intensify the process of heat and mass transfer between solid particles and air flow in vortex chambers. Due to possibility to increase and regulate the time of particle hold-up in the rotating layer and an increase in a relative velocity of particle streamlining by a gas flow, more qualitative drying of loose materials occurs. Combustion of water–coal suspension in the vortex apparatuses seems to be promising. Uncommon properties of interaction between a swirl peripheral jet and axial non-swirling flow are shown brightly in plasma technologies. It is known [1–3] that at some certain flow rate and geometrical parameters, vortex stabilization of plasma filament can be obtained. Simultaneously, the intensity of turbulent mixing between the axial high-temperature flow and peripheral cold jet decreases. This provides an efficient thermal protection for the plasma-chemical reactor.

Complex 3D structure of the swirl flow in a vortex chamber complicates modeling of such class of flows. For numerical analysis of the turbulent swirl flow, it is necessary to obtain the valid description of rotation effect on the averaged and turbulent flow characteristics. The application range of existing approaches [4] using various modifications of the Richardson number is often limited. To check the validity of the chosen model, experimental data on turbulent characteristics of the swirl flow is required. Most publications study the averaged flow characteristics [2].

The work under consideration represents measurement results both for averaged and pulsation flow characteristics in a diaphragm vortex chamber obtained using the two-component laser anemometer.

2. Experimental setup

Experiments were carried out in the vortex chamber shown schematically in Fig. 1. The chamber diameter was 100 mm, and the height was 160 mm. The swirl flow was organized by a swirling device (36 slots with an inclination angle relative to the chamber end surface of 30°) situated on the periphery of chamber bottom. Air ejection from the chamber was performed through a diaphragm hole of the 10 or 20 mm diameter in the upper lid.

Three types of flow in the vortex chamber were considered. For the first type, there were no non-swirling axial jet towards the chamber bottom (Fig. 1a). For the second type, the axial non-swirling air jet was fed through a round hole (Fig. 1b). For the third type of flow, the axial non-swirling air jet was ejected to the chamber bottom through a ring hole of the 1.5 mm width and 20 mm outer

---

* Corresponding authors. Fax: +7-3832-343480.

E-mail addresses: volchkov@itp.nsc.ru (E.P. Volchkov), lebedev@itp.nsc.ru (V.P. Lebedev), luka@itp.nsc.ru (V.V. Lukashov).

doi:10.1016/S0017-9310(03)00399-5

Nomenclature

K	$\frac{\langle u_z\rangle - \langle u_z\rangle}{\langle u_z\rangle + \langle u_z\rangle}$, coefficient of anisotropy
G	air mass rate, g/s
H	height of vortex chamber, mm
r	distance from geometric axis of vortex chamber, mm
$\tilde{r}_0$	$D/2R$, relative radius of diaphragm, dimensionless
$Re_{\varphi K}$	$\frac{\rho U_{\varphi K}}{\mu}$, Reynolds number
Ro	$\frac{F}{R^2 \cos\beta}$, Rossby number
Tu	$\frac{\sqrt{(\overline{u_z'^2} + \overline{u_\varphi'^2})}}{\sqrt{2\cdot(U_z^2 + U_\varphi^2)}}$, level of turbulence
$U_{\varphi K}$	tangential component of velocity at the exit of swirling blages, m/s
U_z	mean axial velocity, m/s
U_φ	mean tangential velocity, m/s
$\langle u_z\rangle$	square mean root of axial velocity fluctuations, m/s
$\langle u_\varphi\rangle$	square mean root of tangential velocity fluctuations, m/s
$\overline{U}_z$	$\frac{U_z - U_z^{\min}}{U_z^{\max} - U_z^{\min}}$, relative axial velocity, dimensionless
$\overline{U}_\varphi$	$U_\varphi/U_\varphi^{\max}$, relative tangential velocity, dimensionless
Δ	distance between diaphragm axis and chamber axis, scaled by diaphragm radius, dimensionless

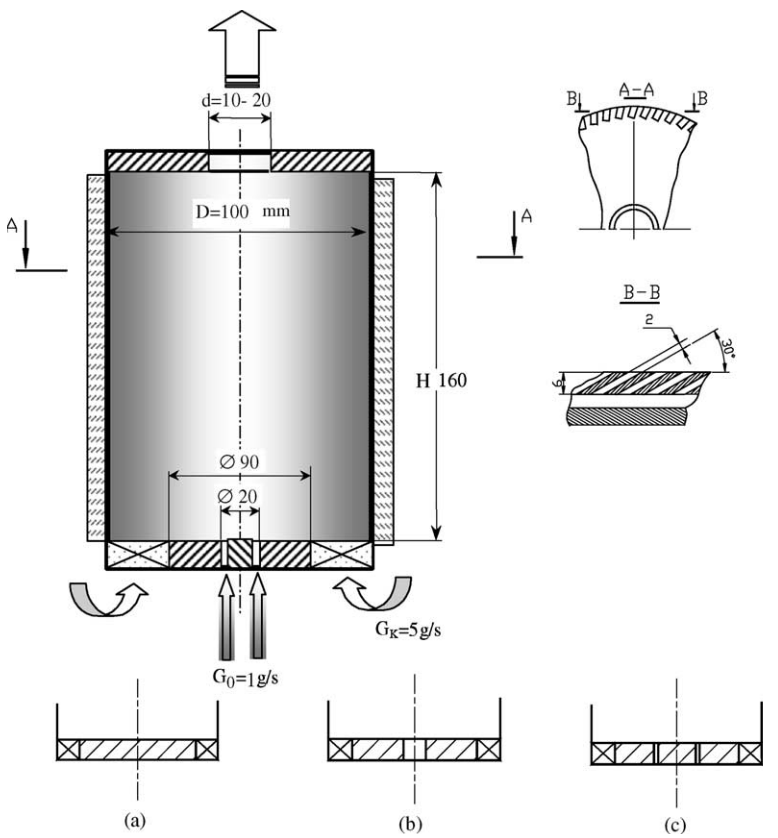

Fig. 1. The scheme of vortex chamber.

diameter (Fig. 1c). As it will be shown below, the arrangement of axial jet did not significantly effect distribution of longitudinal and rotational velocities. Therefore, measurement of gas-dynamic values was

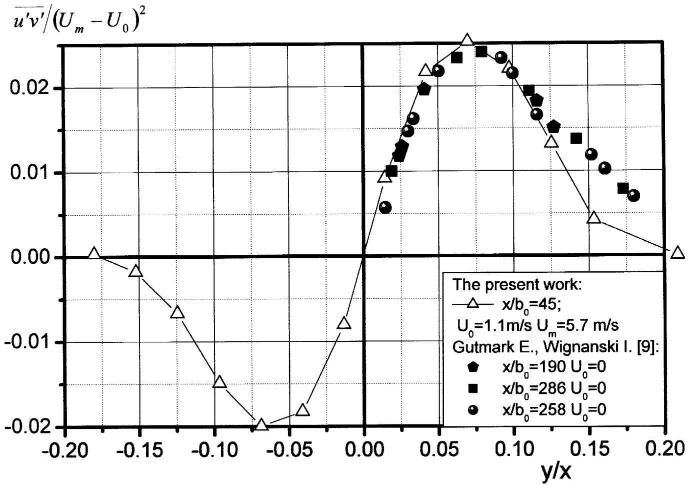

Fig. 2. Testing the LDA system: measurements of cross-correlation in flat jet.

mainly performed for the chamber with an axial non-swirling jet supplied through an annular hole (Fig. 1c). Earlier, this chamber was used in [5] for modeling of heat and mass transfer in the plasma-chemical reactor. Axial and tangential velocity components were measured there by a pneumatic probe in three cross-sections of the chamber. From this point, this chamber is suitable both for research intensification and comparison between new results and data available earlier.

Besides diagnostics of the velocity field, turbulent characteristics of the flow were determined by the work presented. One of the gas-dynamics problems for the swirl flows is the choice of methods for flow diagnostics. Introduction of different pneumatic probes into the flow may provide flow structure destruction and significant distortion of results obtained [6]. Thus, non-contact measurement methods such as the laser Doppler anemometer (LDA) are very promising for the study of complex flows [2]. Measurements were carried out by the two-component laser Doppler anemometer. To avoid distortion of measurement results, caused by interaction between the optic beam and bent surface of cylindrical chamber, a flat optic window of the 27-mm width was mounted into the lateral side of the chamber over its whole height. The two-component LDA with adaptive commutation of the optic channels and reverse scattering was used in experiments [7]. The light source was argon laser LGN-503. The operating power of the emitter was 250–350 mW. The tracking processor "Potok-2" [8] performed the primary treatment of a signal from the photodetector. Particles of glycerin aerosol with the diameter of 1–5 μm were used as the light-scattering centers. The axial and peripheral flows were dusted separately, and this provided more uniform distribution of particles over the chamber. The analogue signal from the outputs of tracking processor was digitized by the multichannel 12-multidigit ADC "Lab-Master" with a frequency of 0.5–5 kHz, the sampling for each of two channels was about 16,000 readings.

The measurement system was tested on well-known types of flows: an annular free jet and a flat co-current jet. The meteorological study allowed determination of demands to operation conditions of the given measurement complex (signal–noise ratio, concentration range of light-scattering particles, parameters of the tracking processor), required for the obtaining of reliable data on turbulence with the error not more than ±5%. The average characteristics were measured with the accuracy of ≈0.5%.

Test results demonstrated perfect coincidence between data measured by laser anemometers and characteristics of the mentioned classical flows. Measured correlation of longitudinal and across velocity pulsation in a flat accompanying flow from [9] is compared with the LDA measurements used in this work in Fig. 2. Results coincide satisfactorily, and this indicates that LDA operates correctly and it can be used for the following studies of the swirl flows.

3. Measurement results

In the current work, the average axial and tangential velocity components measured by the LDA were compared with data from [5], obtained by the pneumatic probe. As it can be seen from Fig. 3, data obtained by the optical (points 1) and probe (points 3) methods coincide satisfactorily, excluding the area adjacent to the geometrical axis of the chamber. Near the swirl axis, measurement results obtained via these two methods diverge significantly, and we can assume that the probe effects the flow.

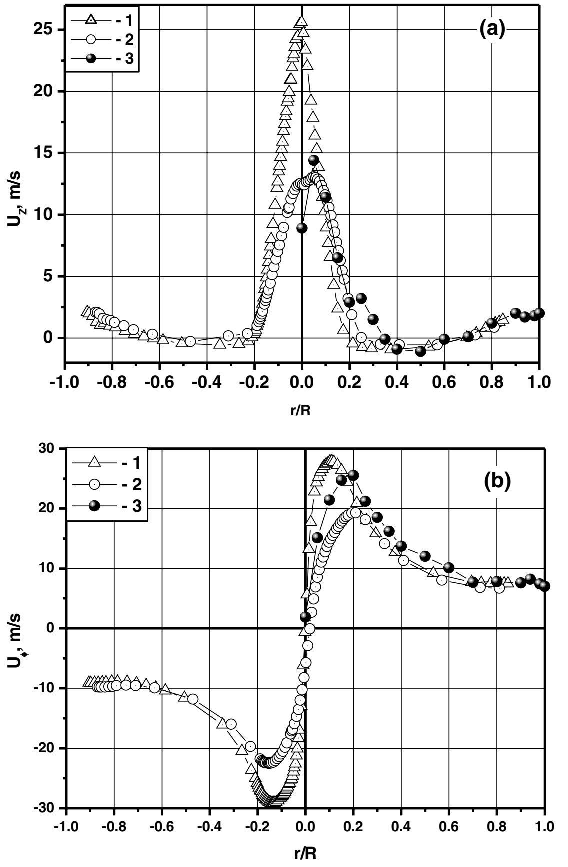

Fig. 3. Mean axial and tangential velocities components of flow. The comparison with the data made by pneumatic probe.

To understand the character of probe effect on the flow pattern, special experiments were carried out. To do this, the wire of the 1.2 mm diameter, which imitated the probe was mounted in the vortex chamber at 5 mm upward the flow from the measurement volume. According to LDA measurements, introduction of this wire into the flow (points 2) decreases velocity U_z by half in the near-axial area in comparison with the case without wire (points 1) (see Fig. 3). It is also obvious from Fig. 3 that in the presence of disturbing wire data from [3], obtained via the pneumatic probe, and LDA measurements coincided. This proves the effect of introduced probe on the flow character in the vortex chamber and necessity to use the non-contact methods for measurements in the swirl flows.

Distribution of the longitudinal velocity over the radius in various cross-sections of the vortex chamber is shown in Fig. 4. According to the diagram, the main flow along the chamber occurs near the axis within the area of ≈1/3 radius. In the rest zone, the longitudinal velocity is close to zero. The maximal value of velocity is at the chamber axis. It is necessary to note that maximal values of axial velocity increase significantly when approaching to the outlet diaphragm. This character of axial velocity alteration is a result of orificing in the outlet cross-section of the vortex chamber: a negative pressure gradient is formed along the axis, and this makes impossible to form the zone of reverse flows at the flow axis.

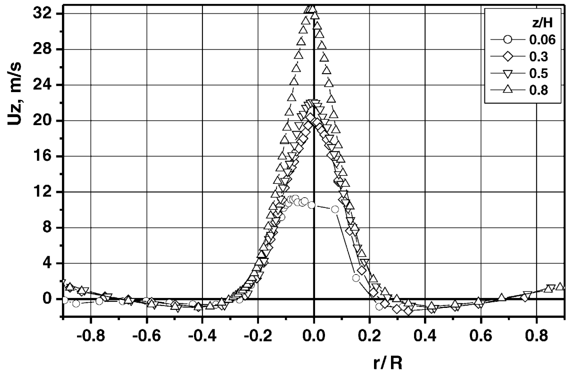

Fig. 4. The distributions of mean axial velocity in vortex chamber.

Axial U_z and tangential U_φ velocities in different chamber cross-sections are self-similar, if they are normalized on their maximal values. This is obvious from Figs. 5 and 6, where $\overline{U}_z = (U_z - U_{z\,\min})/(U_{z\,\max} - U_{z\,\min})$, $\overline{U}_\varphi = (U_\varphi - U_{\varphi\,\min})/(U_{\varphi\,\max} - U_{\varphi\,\min})$. Data obtained for the vortex chambers with injection of the axial jet from a round hole and without it are also shown in these figures. It is clear that for all three variants, distribution of normalized velocities is the same. This allowed us to perform all following investigations using one construction of the chamber bottom.

In the profile of rotating velocity component (Fig. 6), the zero value coincides with the chamber axis, and maximum occurs at $r/R \approx 0.1$–0.2. It is necessary to

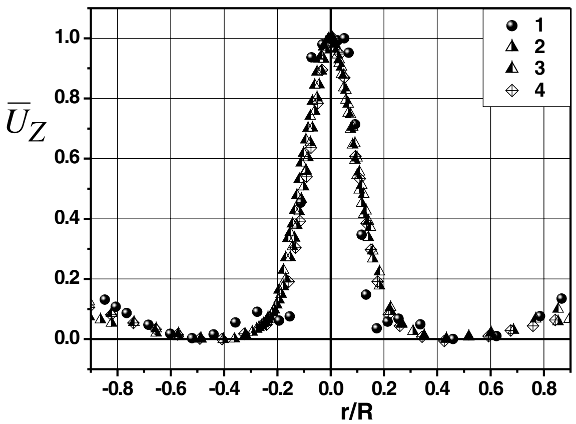

Fig. 5. The dimensionless mean axial velocity profiles.

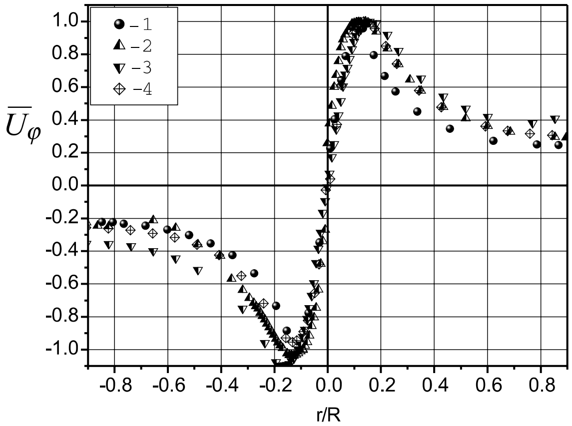

Fig. 6. The dimensionless mean tangential velocity profiles.

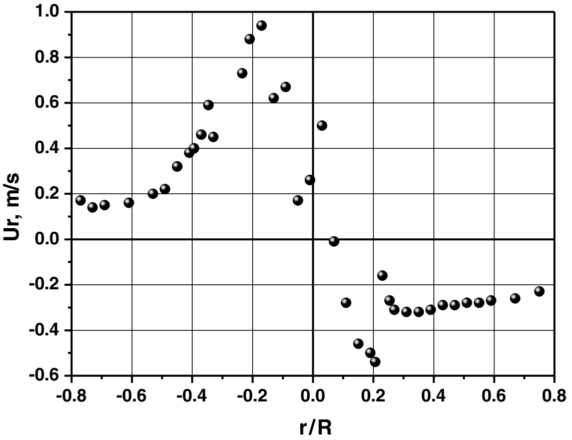

Fig. 8. The mean radial velocity component.

note that in the near-axial area between velocity maximums, velocity distribution is close to the linear one. In other words, there is a zone, which is close to “quazi-solid rotation”. High positive circulation gradients $\Gamma = U_\varphi r$ occur in this zone along radius ($\mathrm{d}\Gamma/\mathrm{d}r > 0$) (Fig. 7), and this characterizes the flow as a stable one. Strong suppression of turbulence should occur in this area, and this will be noted below in the description of measured characteristics of turbulence in the vortex chamber.

Particular problems arose at measurements of the averaged radial velocity component. The plane of velocity measurements should pass the axis of flow rotation in the vortex chamber. A slight inclination of the measurement plane from the axis provided measurement of a portion of rotation velocity. It should be considered that absolute values of radial velocity are low, so slight inclinations from the axis might lead to a significant overestimation of the radial velocity component. After thorough fixation of the coordinate system to the swirl axis, data on distribution of the radial velocity component was obtained. Results are shown in Fig. 8. The criterion, which allows estimate of chamber flowage in the radial direction by the flow rate and geometrical parameters, is presented in [2]. If

$$Re_{\varphi K}^{0.25} Ro^{1.25} < 2.38 \cdot (1 - \tilde{r}_0),$$

$$\text{where } Re_{\varphi K} = \frac{\rho U_{\varphi K} R}{\mu}, \quad Ro = \frac{F}{R^2 \cos\beta},$$

$\tilde{r}_0 = \frac{d}{2R}$ is the ratio of diaphragm diameter to the chamber diameter, so the developed boundary layer is formed on the chamber edge. Beyond this layer, the radial velocity component is close to zero. The flow in radial direction occurs mainly through the end boundary layers. According to estimates, in our experiments this condition is satisfied. Direct measurements of the radial velocity component in cross-section $z/H = 0.5$ (Fig. 8) showed that value U_r did not exceed ~0.9 m/s.

Pulsation components of longitudinal and rotation velocities, used for determination of the flow turbulent characteristics were measured in experiments. Distribution of the turbulence degree over the chamber radius in different cross-sections is shown in Fig. 9. The degree

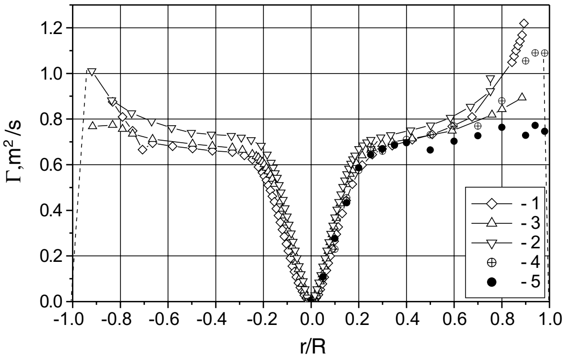

Fig. 7. Circulation in vortex chamber.

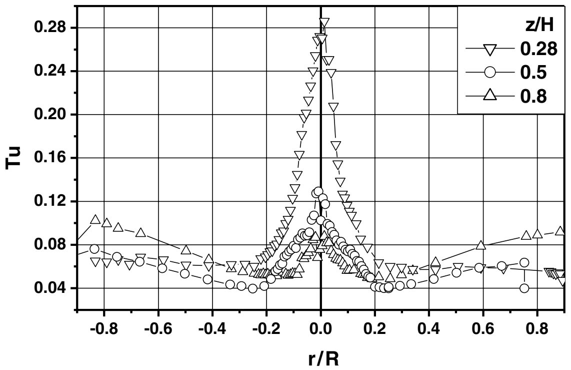

Fig. 9. The turbulence distributions in vortex chamber.

of turbulence was determined via relationship $Tu = \left(\sqrt{(\overline{u_z'^2} + \overline{u_\varphi'^2})/2}\right)/\sqrt{U_z^2 + U_\varphi^2}$. As it can be seen from Fig. 9, two areas corresponding to the axial and peripheral jets are observed in distribution of turbulence degree. These zones differ from each other both by the turbulence level and alteration dynamics over the chamber height. The degree of turbulence in the peripheral area ($r/R > 0.2$) increases with a distance from the flow center from ≈4% to ≈10%. The level of turbulence in cross-section $z/H = 0.8$ is considerably higher than that in cross-section $z/H = 0.28$. In the near-axial area, the level of turbulence is maximal on the chamber axis and falls downward the flow with approach to the outlet diaphragm. As it was mentioned above, there is the maximal positive gradient of circulation along the radius in this area and distribution of rotation velocity is close to velocity distribution at quazi-solid rotation. From this point, we can speak about suppressed turbulence in the field of centrifugal forces (in our experiments, from 28% to 8%). Maximal turbulence of cross-section reduces obviously with approach to the outlet hole, what is shown in Fig. 10, where a change in turbulence degree is demonstrated across the chamber in different cross-sections relative to the initial one. It is also seen from Fig. 10 that boundaries of the axial jet do not change over the chamber height and approximately correspond to the diameter of the outlet diaphragm ($r/R \approx 0.2$).

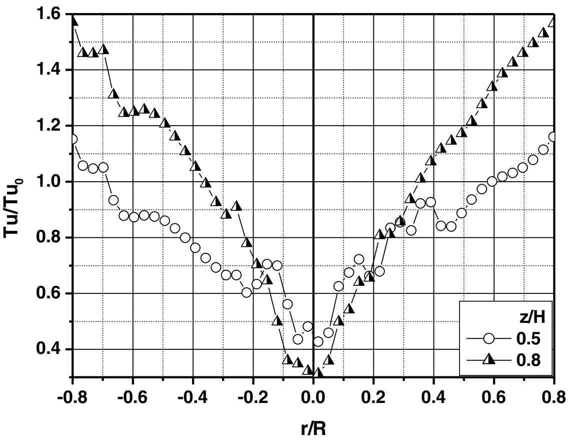

Fig. 10. The turbulence evolution in vortex chamber.

Measurements of velocity pulsation allowed us to determine correlation between the axial and rotation velocities. As the gas density is known (the injected in vortex chamber gas—air), it is possible to define turbulent shear stress $\tau = -\rho\overline{u_z'u_\varphi'}$. Distribution of the turbulent shear stress is shown in Fig. 11. It can be noted that the profiles of turbulent friction take the same form as the profiles of turbulent friction for the case of a free jet. Maximal values of the turbulent shear stress are located approximately at a boundary of mixing between the axial non-swirling jet and the main flow in the chamber. At the periphery, turbulent shear stress τ_T is almost equal to zero in a large area.

Low-frequency oscillations were observed in the near-axial area of the flow in the light of a laser "knife". Perhaps, low-frequency oscillations of the swirl axis occur. These oscillations are close to periodic ones, and a narrow peak in the energy spectrum of axial velocity

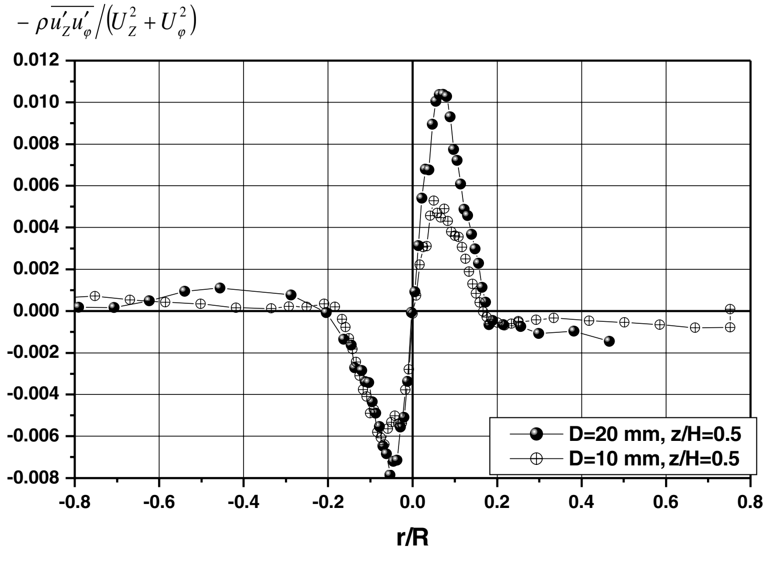

Fig. 11. The cross-correlation in swirling flow of vortex chamber.

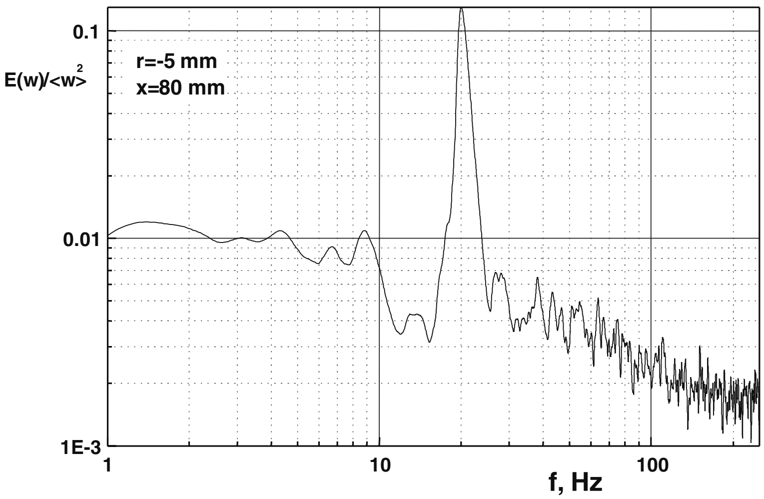

Fig. 12. The reconstructed distribution of mean velocity levels.

pulsation (Fig. 12) proves this. A question about contribution of periodic velocity alteration into the measured value of velocity pulsation arises due to precession. Apparently, precession contribution depends on specific conditions of the flow. For instance, it was obtained in [10] that up to 80% of measured velocity pulsation in the vortex chamber is caused by precession.

In our work, to estimate the effect of quazi-periodic velocity alteration on velocity pulsation obtained in experiments, we used the method of spectral filtration suggested in [11]. The method is based on "triple" expansion of the time series of instantaneous velocities into the average, "periodic" and turbulent components:

$$u(t) = \overline{u} + \tilde{u}(t) + u'(t).$$

The detailed description of the used method of spectral filtration is given in [12]. According to obtained estimates, in our experiments precession contribution into the measured value of velocity pulsation intensity did not exceed 10%.

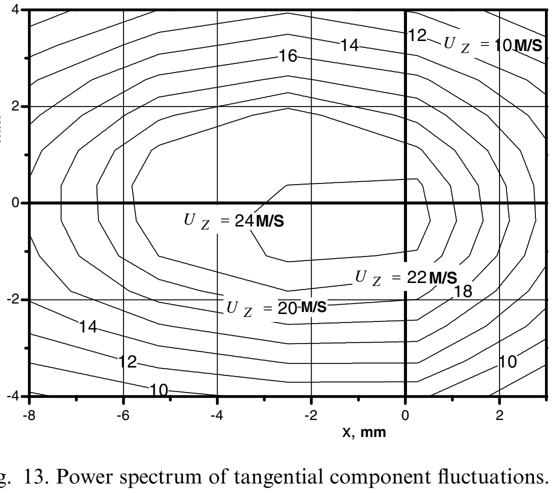

Fig. 13. Power spectrum of tangential component fluctuations.

To get more detailed flow pattern in the near-axial area, the axial velocity component was measured in the middle cross-section of the chamber ($z/H = 0.5$) along five chords and diameter. The obtained set of lines with equal velocities is shown in Fig. 13. It is interesting to note that at precession movement in the swirl flow, the isotach asymmetry is obvious in Fig. 13.

4. Conclusions

The use of non-contact method for flow characteristic measurements (Laser Doppler anemometer) allows significant increase in accuracy of investigations. It is shown that introduction of measurement probes into the swirl flow disturbs the flow pattern and distorts the real flow characteristics.

The averaged axial, rotational and radial velocities were measured in the vortex chamber. It was mentioned that the maximum of axial velocity is on the chamber axis and it increases with approach to the outlet diaphragm. The axial zone of quazi-solid rotation with linear velocity distribution was found in the profile of rotation velocity component. Strong suppression of the initial turbulent jet is observed in this zone. It was shown that axial and rotation velocity components in different cross-sections of the chamber are self-similar, if they are normalized on their maximal values.

Pulsation components of longitudinal and rotation velocities were measured and turbulent flow characteristics were determined. It was defined that the level of turbulence is maximal on the chamber axis and decreases significantly in the axial area downward the flow.

High positive circulation gradients are observed in this area, and this provides suppression of pulsation. Apparently, the high initial level of pulsation intensity is caused by the fact that the studied vortex chamber was blind.

Distribution of the turbulent shear stress over the chamber radius was obtained. It should be noted that the profiles of turbulent friction are similar to the profiles of turbulent friction for the case of a free jet.

Visualization of the flow by a laser "knife", plotting of isotaches of the measured axial velocity and obtained energy spectrum showed existence of swirl axis precession. The effect of quazi-periodic velocity change on measured values of velocity pulsation was estimated by the method of spectral filtration. This effect made up about 10%.

Acknowledgements

The work was supported by the Russian Fund for Basic Research (grants no. 00-15-99090 and 02-02-16170).

References

[1] E.P. Volchkov, The Near-Wall Gas Screens, Nauka, Novosibirsk, 1983, 240 p.

[2] S.S. Kutateladze, E.P. Volchkov, V.I. Terekhov, Aerodynamics and Heat and Mass Transfer in the Limited Swirl Flows, Novosibirsk, 1987, 282 p.

[3] E.P. Volchkov, A.I. Leontiev, V.P. Lebedev, et al., Thermal Protection of Plasmatron Walls, Novosibirsk, 1995, Low-Temp. Plasma 15, 332 p.

[4] D.G. Sloan, P.J. Smith, L.D. Smoot, Modeling of swirl in turbulent flow systems, Prog. Energy Combust. Sci. 12 (1986) 163–250.

[5] E.P. Volchkov, V.I. Terekhov, Yu.N. Tkach, Experimental study of mixing between an axial jet and peripheral flow in the vortex chamber, Preprint of ITP 124-85, Novosibirsk, 1985.

[6] I.I. Smulsky, Concerning peculiarities of velocity and pressure measurements in the vortex chamber, Thermal Physics and Physical Hydrodynamics, Novosibirsk, 1978, pp. 125–132.

[7] Yu.N. Dubnishev, V.G. Belousov, V.A. Pavlov, V.G. Meledin, Laser Doppler anemometer with adaptive temporal selection of the velocity vector, Opt. Appl. 20 (3) (1990).

[8] Yu.G. Vasilenko, V.A. Gavrilov, V.N. Grigoriev, E.V. Kozhukhova, E.V. Sysoev, V.I. Titkov, Laser Doppler anemometer "Potok-1" with programmable operation regimes, The First All-Union Seminar Optic methods for flow investigations, Novosibirsk, 1989, p. 11.

[9] E. Gutmark, I. Wignanski, The planar turbulent jet, J. Fluid Mech. 73 (1976) 3.

[10] N. Grosjean, L. Graftieaux, M. Michard, W. Hubner, C. Tropea, J. Volkert, Combining LDA and PIV for turbulence measurements in unsteady swirling, Meas. Sci. Technol. 8 (12) (1997).

[11] G.J. Brereton, A.A. Kodal, Frequency-domain filtering technique for triple decomposition of unsteady turbulent flow, Trans. ASME 46 (114) (1992) 45–50.

[12] R.Kh. Abdrakhmanov, V.V. Lukashov, Experimental study of turbulent characteristics of the swirl flow in a "cold" model of the swirl plasmochemical reactor, Physical fundamentals of experimental and mathematical modeling of gas-dynamics, heat and mass transfer in power installations, The XIII school-seminar of young scientists and specialists headed by Acad. of RAS A.I. Leontiev, St-Petersburg, vol. 1, 2001, pp. 104–107.